Snail Trails and Cell Microcrack Impact on PV Module Maximum Power and Energy Production

Alberto Dolara, *Member, IEEE*, George Cristian Lazaroiu, *Senior Member, IEEE*, Sonia Leva, *Senior Member, IEEE*, Giampaolo Manzolini, and Luca Votta

***Abstract*—This paper analyzes the impact of the snail trail phenomena on photovoltaic (PV) module performances and energy production. Several tests (visual inspection, maximum power determination, dielectric withstand, wet leakage current, and electroluminescence test) were carried out on 31 PV modules located in a PV plant in Italy. The electroluminescence test highlighted the strong correlation between the appearance of snail trails and presence of damaged cells in PV modules. The daily energy produced by four PV modules affected by snail trails ranged between 68% and 88% of the energy produced by a damage free commercial PV module over the same period.**

***Index Terms*—Electroluminescence (EL), microcracks, photovoltaic (PV) modules, PV system reliability, snail trail phenomena.**

I. Introduction

THE direct use of solar energy for electrical energy production faced an intense development due to ongoing CO_2 emission reduction policies and the significant technical developments of photovoltaic (PV) technology. In addition, over the past decade, the cost production of PV cells has dropped, making electricity costs closer to conventional fuel costs. This development requires detailed evaluation of PV performances over lifetime to identify potential degradation phenomena [1]. Examples of degradation phenomena occurring in operating PV systems are encapsulant browning, delamination and bubble formation in the encapsulant, back sheet polymer cracks, front surface soiling, blackening at the bottom edge of the module, junction box connections corrosion, busbar oxidation and discoloration, junction cables insulation degradation, and glass breakage [2]–[4].

Among these, over the past few years, the "snail trails" (also known as worm marks or snail tracks) have been increasingly occurring in PV systems within few months after the installation. These effects appear on the front side or the edge of the solar cells [5], [6], such as a small narrow dark line and discoloration on the surface of the cell, [7], [8].

Manuscript received March 15, 2016; revised May 20, 2016; accepted May 25, 2016.

A. Dolara, S. Leva, and G. Manzolini are with the Department of Energy, Politecnico di Milano, Milano 20133, Italy (e-mail: alberto.dolara@polimi.it; sonia.leva@polimi.it; giampaolo.manzolini@polimi.it).

G. C. Lazaroiu is with the Department of Power Systems, Politehnica University of Bucharest, Bucuresti 060042, Romania (e-mail: cristian.lazaroiu@upb.ro).

L. Votta is with Kiwa Cermet Italia, 40057, Cadriano di Granarolo Emilia, Italy (e-mail: luca.votta@kiwacermet.it).

Color versions of one or more of the figures in this paper are available online at http://ieeexplore.ieee.org.

Digital Object Identifier 10.1109/JPHOTOV.2016.2576682

In previous works, the correlation between snail trail discolorations within the cells and cell microcracks was demonstrated. Meyer *et al.* performed chemical tests, Fourier transform infrared investigations, and X-ray photoelectron spectroscopy measurements on PV modules for snail trail defect analysis. Snail trails were correlated with chemical reactions occurring between silver of grid fingers and air humidity [5], [8]–[12].

Köntges *et al.* used fluorescence radiation to investigate micro cracks in PV cells, in order to determine the number, the position/orientation, and the frequency [13], [14]. Studies were further carried out in [15], simulating the PV module power affected by different crack types. The authors estimated that cracks isolate a cell section leading to a module strings power loss around 6–22%. They also suggested that the replacement of the most damaged module in a string allows a power recovery lower than the nominal power of a new module.

In [16], experiments to evaluate the impact of discolored lines like snail trails were performed both in laboratory and outdoor field, together with aging tests. A power reduction exceeding 5% was measured, and it was related to cell microcrack before snail trail formation.

This paper is a follow-up of a previous work [17] and investigates the performance of 31 PV modules under operation in a PV plant in Italy. The modules considered in this paper include also the four PV modules monitored in [17], where outdoor experiments on PV panels affected by snail trails outlined a reduction 1) in the photogenerated current, 2) of the shunt resistance in the electric equivalent circuit, and 3) of the energy production by 35%. Due to absence of some tests, no ultimate conclusions on the correlation between the snail trails phenomena and cells microcrack could be extended.

In this paper, several additional analyses were performed to highlight eventual issues besides visual defects as discoloration. The analyses are indoor visual inspection, maximum power determination, MST16 dielectric withstand, and wet leakage current. An important test carried out was the electroluminescence (EL) one, which allows correlating inactive ("broken") cell area and the level of performance loss. After the initial screening, the same modules considered in [17] were evaluated with long outdoor testing lasting five months 1) to compare the power and energy performances after two additional years of operation and 2) to assess the long-term behavior of cell cracks or snail trails under real operating conditions. The long-term observation of modules with grid finger discoloration is really a new contribution to this work, which, to the knowledge of the authors, was not previously investigated.

The experimental measurements were carried out at SolarTech^{LAB} [18], Politecnico di Milano, Italy.

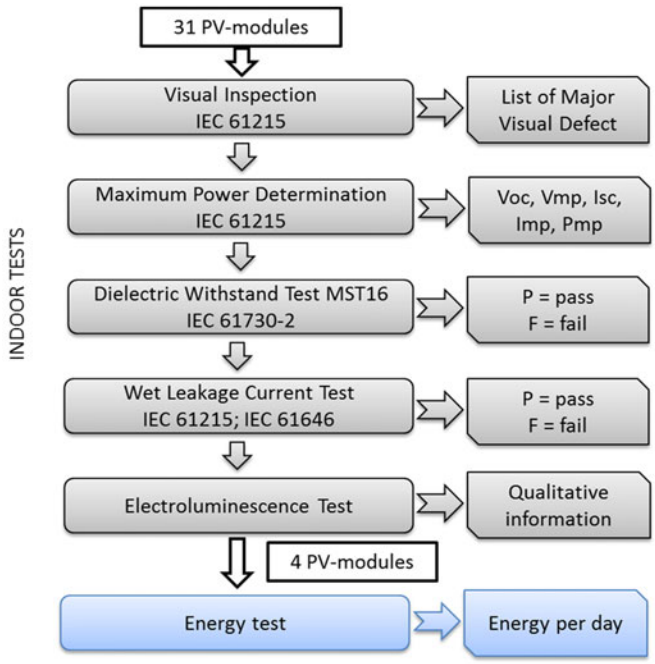

Fig. 1. Experimental procedure flowchart.

The paper is organized as follows: Section II describes the experimental procedures and the conducted tests. Section III reports the indoor experimental results, while Section IV reveals the energy experimental results for assessing snail trails effects on PV performances. In Section V, a comparison between the old and new outdoor measurements is presented. Section VI reports the final conclusions and the discussion of obtained results.

II. Experimental Procedure

The modules considered in this study were taken from a PV plant in operation. Among 4000 PV modules installed, 31 were selected by visual inspection: 16 modules affected by the snail trails at different rates and 15 with no trace of degradation.

As mentioned in [17], all the modules were manufactured in 2011 and have been operating since early 2012. Before their installation, each module performance was measured revealing good agreement with the corresponding datasheet, and no snail trail phenomenon or other issues were identified. After less than six months, these PV modules started to report a performance decay correlated with snail trail formation, since neither damages nor artificial breakage occurred. Performance decay was first evaluated in 2013 and, then, in 2015. During 2013–2015, the PV modules were in operation.

A multistep procedure (summarized in Fig. 1) was defined to assess the status and performances of the 31 modules. The procedure can be divided into two phases: the first one, named indoor tests, was carried out for all the modules, and the second one, named outdoor tests, for a limited number of modules. The following analyses were carried out.

A. Visual Inspection Tests

Visual inspection tests have been performed as defined by IEC 61215 [19]. For the purposes of design qualification and type approval, major visual defects were considered to be the following:

1) broken, cracked, or torn external surfaces, including superstrates, substrates, frames, and junction boxes;
2) bent or misaligned external surfaces, including superstrates, substrates, frames, and junction boxes to the extent that the installation and/or operation of the module would be impaired;
3) cracks, bubbles, or delaminations forming a continuous path between any part of the electrical circuit and the edge of the module;
4) loss of mechanical integrity, to the extent that the installation and/or operation of the module would be impaired.

B. Maximum Power Determination

The *I–V* characteristic curves were traced at standard test conditions (STC) in a sun simulator chamber of class AAA and *I–V* curve generator as defined by IEC 61215 [19]. The obtained results, at STC, were the following:

1) the open-circuit voltage V_{OC};
2) the voltage at maximum power point (MPP) V_{MPP};
3) the short-circuit current I_{SC};
4) the current at MPP I_{MPP};
5) the power at MPP P_{MPP}.

Using the maximum power value, the power variation (EFF) with respect to the nominal power value (i.e., indicated in the PV module datasheet) was calculated as follows:

$$\mathrm{EFF} = \frac{P_{\mathrm{MPP}} - P_N}{P_N} \cdot 100. \quad (1)$$

A negative value of EFF means a reduction in the power production with respect to the datasheet nominal power indicating possible problem in the module.

During MPP determination and EL tests, the electrical wires, connections, as well as the junction box or bypass diodes were also investigated to certify that they are undamaged and correctly operating.

C. MST16 Dielectric Withstand Test

This test is carried on at ambient temperature, according to the standard IEC 61730-2 [20], and at relative humidity not exceeding 75%. The module passes the test if there is no evidence of dielectric breakdown, or surface tracking, when a voltage equal to 2000 V plus four times the maximum voltage system is applied.

D. Wet Leakage Current Test

In agreement with the standards IEC 61215 [19] and IEC 61646 [21], the sample passes the test if the measured insulation resistance multiplied by the area of the module shall not be below 40 MΩ·m^2 (for modules with an area higher than 0.1 m^2).

TABLE I
OBTAINED RESULTS BY VISUAL INSPECTION AND MAXIMUM POWER DETERMINATION

#	P_N (W)	Finding – description	V_{OC} (V)	V_{MPP} (V)	I_{SC} (A)	I_{MPP} (A)	P_{MPP} (W)	*EFF*
1	220	Fingers blackened, scratch on cell, mark on cell. No major visual defects	24.5	19.7	8.25	7.53	148.4	-32.55%
2	220	Fingers blackened. No major visual effects	36.29	29.23	8.22	7.6	222	0.91%
3	230	Mark on cells, crack. No major visual defects	36.98	30.11	8.19	7.55	227.4	-1.13%
4	220	Fingers blackened. No major visual defects	36.35	29.17	8.25	7.57	220.7	0.32%
5	220	Fingers blackened. No major visual defects	36.27	29.18	8.18	7.59	221.4	0.64%
6	220	Mark on cells. Finger blackened. No major visual defects	36.35	29.24	8.16	7.71	225.3	2.41%
7	220	Fingers blackened. No major visual defects	24.09	19.42	8.23	7.59	147.3	-33.05%
8	220	Fingers blackened. No major visual defects	36.35	29.83	8.27	7.62	227.2	3.27%
9	220	Mark on cell. Fingers blackened. No major visual defects	36.32	29.23	8.34	7.69	224.8	2.18%
10	230	Fingers blackened, scratch on cell. No major visual defects	36.48	29.81	8.05	7.41	220.9	-3.96%
11	230	Fingers blackened. No major visual defects	36.87	30.18	8.28	7.68	231.8	0.78%
12	230	Scratch on cell. Finger blackened. No major visual defects	36.41	29.25	8.34	7.81	228.5	-0.65%
13	230	Fingers blackened. No major visual defects	36.39	29.87	8.2	7.53	224.9	-2.22%
14	230	Mark on cells. Fingers blackened. No major visual defects	36.48	29.25	8.29	7.88	230.5	0.22%
15	230	Mark on cell. Fingers blackened. Scratch on cells. No major visual defects	36.49	28.93	8.2	7.69	222.5	-3.26%
16	220	Several Snail Trails. Evidence of burning on cells and fingers	36.65	27.8	8.09	7.03	195.5	-11.14%
17	220	Several Snail Trails. Fingers blackened. Evidence of burning on cells	36.81	28.21	8	5.73	161.6	-26.55%
18	220	Several Snail Trails. Fingers blackened. Evidence of burning on cells	36.8	28.46	7.63	5.66	161.2	-26.73%
19	220	Several Snail Trails. Evidence of burning on cells. Fingers blackened	36.5	28.67	7.94	6.68	191.5	-12.95%
20	220	Evidence of burning on cells. Diverse snail trails. Fingers blackened	36.53	28.7	8.18	6.93	198.9	-9.59%
21	220	Several Snail Trails. Evidence of burning on cells. Fingers blackened	36.64	28.62	7.75	6.6	188.7	-14.23%
22	220	Several Snail Trails. Evidence of burning on cells	36.47	28.74	8.05	6.83	196.3	-10.77%
23	220	Several Snail Trails. Evidence of burning on cells. Fingers blackened	36.68	28.54	8.03	5.96	170.1	-22.68%
24	220	Several Snail Trails. Evidence of burning on cells. Fingers blackened	36.14	27.67	8.21	6.21	171.8	-21.91%
25	220	Several Snail Trails. Evidence of burning on cells. Fingers blackened	36.4	28.62	8.02	6.66	190.7	-13.32%
26	220	Several Snail Trails. Evidence of burning on cells. fingers blackened	36.47	28.64	8.07	6.41	183.5	-16.59%
27	220	Several Snail Trails. Evidence of burning on cells. Fingers blackened	36.52	28.78	7.94	5.82	167.5	-23.86%
28	220	Several Snail Trails. Evidence of burning on cells. fingers blackened	36.55	28.99	8.14	6.88	199.6	-9.27%
29	220	Several Snail Trails. Evidence of burning on cells. Fingers blackened	36.53	28.68	8.11	6.74	193.3	-12.14%
30	230	Evidence of burning on cells e Several Snail Trails	36.41	28.77	8.07	7.14	205.3	-10.74%
31	220	Several Snail Trails. Evidence of burning on cells. Fingers blackened. Cell chipped	36.69	27.39	8.16	6.48	177.4	-19.36%

E. Electroluminescence Test

The EL test is a qualitative test used, in particular, for detecting microcracks in PV modules. The affected areas are darker as they emit low or do not generate light emission. Thus, microcracks that are not visible, as well as broken contact fingers, can be identified. Sometimes, this test cannot be applicable (N/A) due to connection problems within the modules. In addition, for cracks not affecting the entire cell, future issues can be estimated if the module is further stressed (i.e., cracks electrically separating the major part of the cell) [1], [13], [14].

F. Energy Test

Four PV modules chosen among the ones with the lowest EFF were then analyzed under actual environmental conditions at the SolarTech$^{\text{LAB}}$ [18]. The irradiance availability in the site is calculated in terms of daily reference yield ($Y_{r,d}$). The energy produced by these PV modules was evaluated in terms of daily final yield index ($Y_{f,d}$) [22] and relative daily final yield ($RY_{f,d}$).

In agreement with the IEC 61724 [23], the daily reference yield $Y_{r,d}$ represents the number of peak sun-hours and is calculated as the global horizontal irradiance (GHI) in a day (kW h/m^2) divided by the reference irradiance (1 kW/m^2):

$$Y_{r,d} = \frac{\mathrm{GHI}_d(\mathrm{kWh/m^2})}{1(\mathrm{kW/m^2})}. \tag{2}$$

The index $Y_{f,d}$ is the energy output of the system divided by the peak power of the installed PV array at STC:

$$Y_{f,d} = \frac{E_{\mathrm{out},d}(\mathrm{kWh})}{P_N(\mathrm{kW})}. \tag{3}$$

The relative daily final yield is defined as the ratio between the final yield $Y_{f,d}$ of the PV modules under investigation, and the final yield $Y_{f,d\mathrm{REF}}$ of reference PV module:

$$RY_{f,d} = \frac{Y_{f,d}}{Y_{f,d\mathrm{REF}}} \cdot 100. \tag{4}$$

III. INDOOR EXPERIMENTAL TESTS RESULTS

The obtained results of the visual inspection and maximum power determination tests are summarized in Table I (the color label represents the difference between the PV module maximum power and the datasheet value: green indicates a positive or slight difference while red the highest power reduction). The PV modules #1 – #15 did not show significant visual defects. Indeed, no variation of maximum power of PV modules was measured, but for modules #1 and #7 which show a power reduction of about 33%. A further analysis related this reduction to some defects in the junction box connections, where one third of the module is disconnected and does not generate energy. The PV modules #16 – #31 had several snail trails deeply analyzed by EL tests with some fingers blackened in all the modules. Every module with discoloration due to snail trails has an MPP

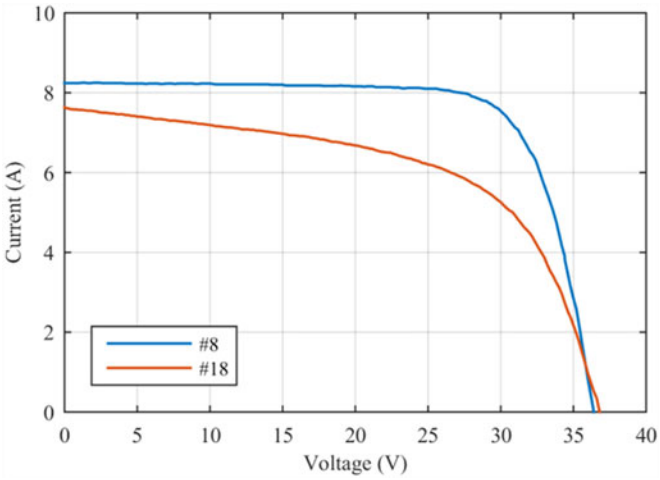

Fig. 2. Measured *I–V* curves of PV modules without major visual defects (#8) and with several snail trails (#18).

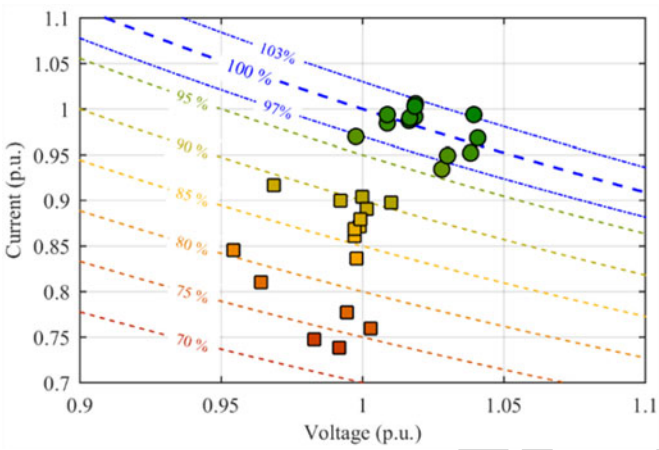

Fig. 3. MPP of the PV modules under analysis (except the one affected by diode failure) measured at STC in comparison with datasheet value (100%).

value below the nominal power; the reduction ranges from -9% to -27% with respect to the nominal power available from the datasheet.[1] In particular, a decay of the current at MPP can be outlined, while the I_{SC} and voltages are only marginally affected.

In Fig. 2, the measured *I–V* curves of two PV modules #8 and #18 are reported. The two curves show significant differences in the MPP, as well as resistance values: the shunt and series resistances in the equivalent electric circuit derived for the PV module #8 are 332.8 Ω, respectively, 0.4 Ω. For the PV module #18, the shunt resistance reduces to 23.6 Ω and the series resistance increases to 0.8 Ω. This is in agreement with the results reported in [17]. The same trend was outlined also for all the other modules affected by microcracks, but the graphs are not reported here for the sake of brevity.

Fig. 3 summarizes the voltage and current at MPP referred to the values indicated on the datasheet of the PV module.

[1]Some discrepancies occur between P_{MPP} reduction determined in this paper and in [17]. This may be due to the different adopted instrumentation, as well as test conditions (outdoor versus indoor).

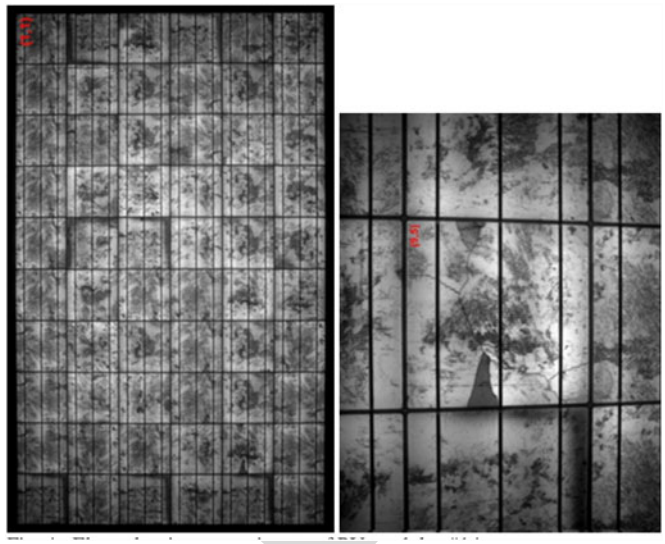

Fig. 4. EL image of PV modules #14.

The dashed lines are percentages of the maximum power. The modules not affected by snail trails are between or close to the blue-dashed lines, which represent the nominal power output $\pm 3\%$ of tolerance. Modules with snail trails have power output ranging from 75% to 90% of the nominal ones, which is mainly due to current density reduction.

In addition, all PV modules complied with the dielectric withstand test and wet leakage current test. Thus, there are no major anomalies in the electrical insulation of investigated PV modules, in dry and humid environment.

The last indoor test was the EL which was performed on all the modules. As a term of comparison, the EL image of a PV module without visual defects (#14) is reported in Fig. 4.

Among the 16 modules affected by snail trails, four among the ones with the lowest EFF were selected for the energy test at SolarTech$^{\mathrm{Lab}}$. The selected modules are #17, #18, #23, and #24 whose EL results are reported in Fig. 3, together with their visual imagery. Black areas in EL images represent electrically separated sections. The positions of cell are indicated in terms of coordinate (row, column) within the PV module, e.g., position (1,1) is on the left, top.

Starting from PV module #17, several snail trails are visible, e.g., in positions (3,1), (4,1), and (5,1). Furthermore, cracks are distinguishable in some cells located in positions (6,3) and (10,2). In addition, poor finger contacts are visible [see cell (5,4)]. Same considerations can be extended to the module #18 and #24, where snail trails are visible in cells (2,1), (2,2), and (3,3) in #18, while in #24, they are located in positions from (1,2) to (6,2). In addition, in these cases, poor finger contacts are present in cell (4,4) and position (6,1) and (7,1) in #18 and in #24, respectively.

In the case of PV module #23, several snail trails are visible, e.g., in position (1,5), (1,6), and (1,7); these correspond to electrically separated areas in EL images. Furthermore, cracks are distinguishable in some cells, e.g., in position (5,3). Again, poor finger contacts are visible, e.g., on cell (5,4), and not uniformity in light is present, e.g., on cells (7,4) and (5.3). For the module

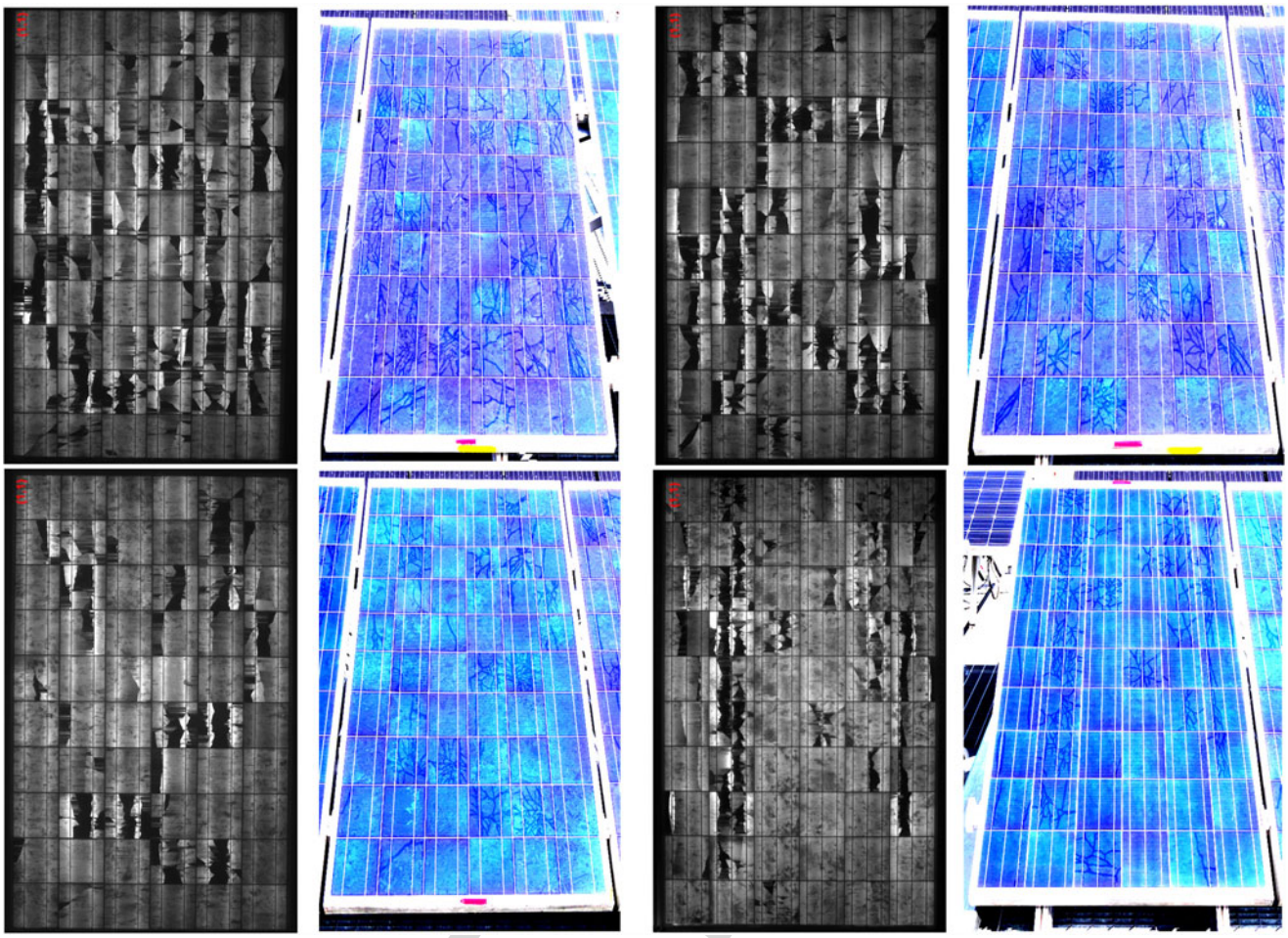

Fig. 5. EL image and picture of PV modules #17, #18, #23, and #24 starting from top-left.

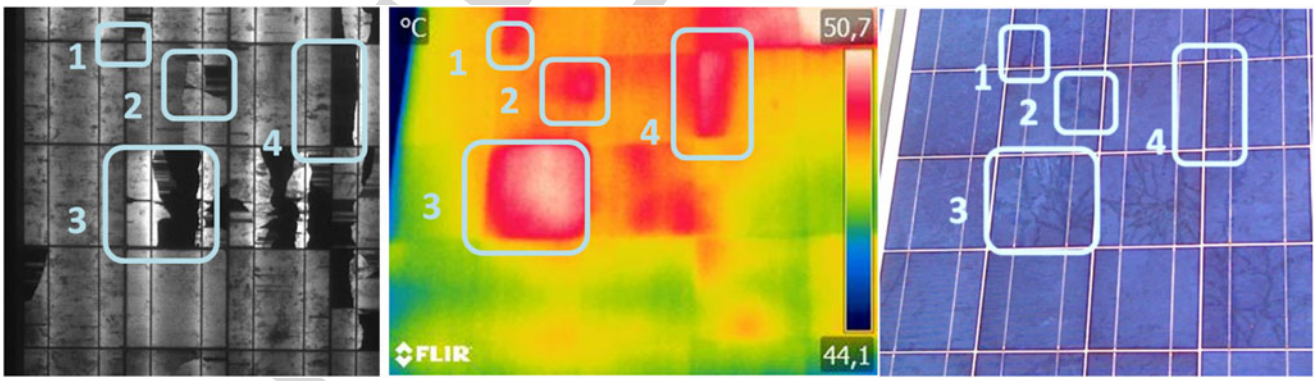

Fig. 6. EL, thermal, and visual imagines of #23 PV-module from (7,1) to (9,3) cells.

#23, in addition to EL analysis which outlined the same issues of the previous models, a thermal image together with EL and visual images of cells from (7,1) to (9,3) cells are shown in Fig. 4. Comparing the three images, it is possible to identify a link among visual defects, hot parts, and electrically separated areas.

In conclusion, the visual inspection carried on for all analyzed PV modules revealed the existence of various failures for 16 of them (#16 to #31), definitely ascribable to the phenomena known as "snail trails" on the PV modules under test. The EL test reveals the strong correlation between the appearance of snail trails and presence of damaged cells (microcracks) in PV modules. In addition, based on the experimental tests regarding determination of MPP, PV modules with significant cell breakage have a power reduction by 26–27% calculated at STC with respect to the manufacturer datasheet data.

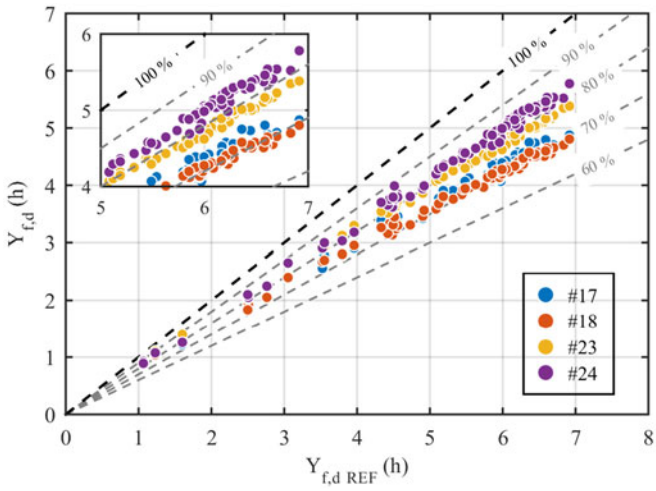

Fig. 7. Daily final yield of the PV modules #17, 18, 23, and 24 in the period April 2015–August 2015 referred to the daily final yield of the reference PV modules.

IV. Energy Comparison in SolarTech^{Lab}

An experimental campaign to evaluate the impact of snail trails on the energy production by PV modules was carried out. The objective of this experimental analysis was to assess the energy reduction due to snail trails and cell cracks phenomenon in some PV modules. MPP reduction is an indication about module performances at only one condition, while long-term energy analysis provides more insight about the status of the module affected by snail trails. In addition, the energy analysis is used to compare the module performance with previous results reported in [17]. The analysis focused on the total energy production over a period of four months.

The four PV modules #17, #18, #23, and #24 were installed at SolarTech^{Lab} [18] together with a commercial PV module (REFPV) of the same technology used as a reference case. The difference in aging was taken into account according to the datasheet information of the PV modules.

The continuous monitoring of the PV modules was conducted using the microinverter configuration adopted at the SolarTech^{Lab}. The inverters were previously characterized in terms of efficiency at different operating conditions, revealing a quite uniform behavior. Therefore, a possible performance reduction of the analyzed plant could specifically be related to the PV module and not to the power conversion system.

The energy produced by the PV modules in the period from April 2015 to August 2015 was recorded to quantify the influence of snail trails/cracks in terms of daily and total energy within the conducted test period. The daily energy generation—in terms of final yield ($Y_{f,d}$)—by PV modules referred to the final yield of REFPV module ($Y_{f,d\mathrm{REF}}$) is summarized in Fig. 7. The energy generation of the REFPV module, in terms of equivalent hours at peak power, is the black-dashed line.

The daily charts prove that the four PV modules affected by snail trails have a lower final yield ($Y_{f,d}$) between 68% and 88% with respect to the REFPV module. Since the reduction is referred to a PV module installed in the laboratory, the decrease can be related to the snail trails phenomenon due to microcrack. Hence, microcracks affect the PV performances by reducing the electrical energy production.

Fig. 8 illustrates the variation of relative daily final yield index ($RY_{f,d}$) for the four affected PV modules (#17, #18, #23, and #24) for each measured day. As illustrated in Fig. 8, the performance decay is higher during high solar radiation days characterized by high $Y_{r,d}$. Table II summarizes the final yield and relative final yield for the different months and the entire period of analysis. It is important to underline that the numbers of days in which the data are available are different for each month. PV modules #17 and #18 presents the highest reduction in energy production by about 30% than the REFPV module. Modules #23 and #24 show a lower energy reduction: they produce about 20% less in term of energy than the REFPV. These results are similar to the ones obtained by the maximum power tests. Besides diverse measurement accuracies and references adopted (REFPV instead of datasheet), the energy analysis represent the average behavior of the module under real operating conditions, which can differ from the ones at MPP. The energy results outline that the average behavior cannot be easily predicted: two modules (#17 and #18) have an energy reduction higher than the one at MPP, while the opposite occurs for #23 and #24.

Finally, the indoor measurements are carried out at STC, while the outdoor measurements are made under real conditions and, hence, affected by variable weather.

V. Long-Term Behavior of Snail Trails

An additional comparison in terms of energy production and visual analysis between previous [17] and this work is carried out to assess the long-term reliability of PV modules affected by snail trails. The four PV modules under analysis in the period in between operated for a total in-plane solar insolation of about 2000 kWh/m^2; hence, they suffered aging by actual weather conditions (sun UV, rain, snowfalls, etc.).

Table III summarizes the energy production results in terms of RY_{F} index obtained in the two campaigns. No significant deviation in the behavior of the PV modules can be outlined. The small differences can be due to different duration of the measurement campaigns and to diverse weather conditions.

Furthermore, a comparison in terms of visual images was performed. The PV cell visual inspection outlined only minor variations from 2013 to 2015. In general, only one or two cells in each PV module showed new snail trails, affecting a very limited area of the PV cell. This can be seen in Fig. 9, where in 2015, a small defect, which was not present in 2013, has appeared in the bottom right area of the PV cell.

Moreover, only in a few cells of each module, a variation of the fingers close to the snail trails was observed moving from case a to case b.

1) *Case a:* Fingers are not interrupted, and there is only a color variation from metallic gray to black [see Fig. 10(a)].
2) *Case b:* Fingers look broken, and small metal agglomerates with spherical shape are present in the center of the finger [see Fig. 10(b)].

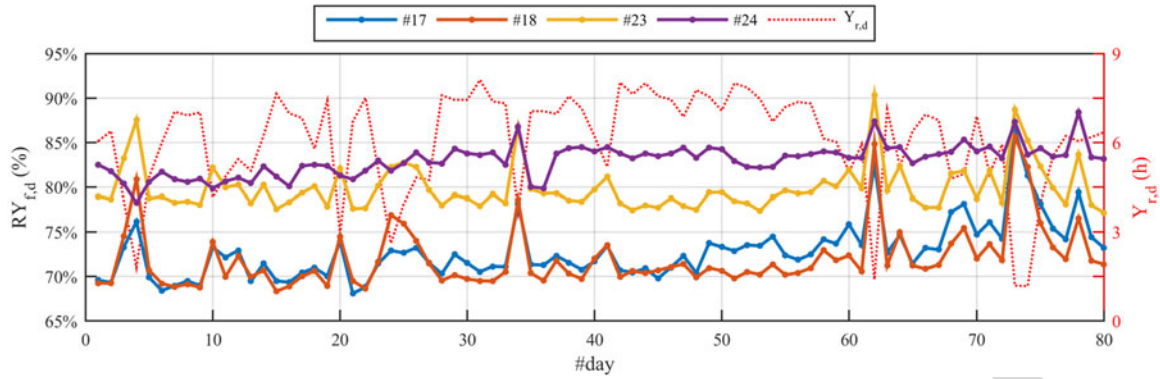

Fig. 8. Relative daily final yield index of the four PV affected modules #17, #18, #23, and #24 for 80 days in the period of analysis. The daily reference yield index for the same days has been reported on the secondarary *y*-axes.

TABLE II
MOTHLY AND TOTAL FINAL YIELD INDEX ($Y_{f,m}$) AND RELATIVE FINAL YIELD INDEX ($RY_{f,m}$) OF THE #17, #18, #23, AND #24 PV MODULES AND THE REFERENCE MODULE

			REFPV	#17		#18		#23		#24	
Month	Number of considered days	Solar irradiance (Wh/m^2)	$Y_{f,m}$ (h)	$Y_{f,m}$ (h)	$RY_{f,m}$	$Y_{f,m}$ (h)	$RY_{f,m}$	$Y_{f,m}$ (h)	$RY_{f,m}$	$Y_{f,m}$ (h)	$RY_{f,m}$
April	9	50.11	48.47	33.82	69.8%	33.96	70.1%	38.41	79.2%	39.31	81.1%
May	25	147.79	130.66	92.94	71.1%	92.43	70.7%	103.75	79.4%	107.59	82.3%
June	14	100.52	84.15	59.93	71.2%	59.52	70.7%	66.16	78.6%	70.12	83.3%
July	13	89.66	75.28	55.27	73.4%	53.38	70.9%	59.73	79.3%	62.72	83.3%
August	19	97.96	85.85	64.41	75.0%	62.77	73.1%	68.57	79.9%	72.22	84.1%
TOTAL	80	486.05	424.42	306.37	72.2%	302.05	71.2%	336.62	79.3%	351.96	82.9%

TABLE III
RELATIVE FINAL YIELD INDEX (RY_f) OF THE FOUR PV MODULES AFFECTED BY SNAIL TRAILS PHENOMENA FOR THE OLD AND NEW OUTDOOR MEASUREMENTS

PV Module	RY$_f$ [17][a] August 2013	RY_f April–August 2015
#17	68%	72%
#18	71%	71%
#23	77%	79%
#24	84%	83%

[A] RY_F was not adopted in [17]; hence, it was calculated starting from published numbers.

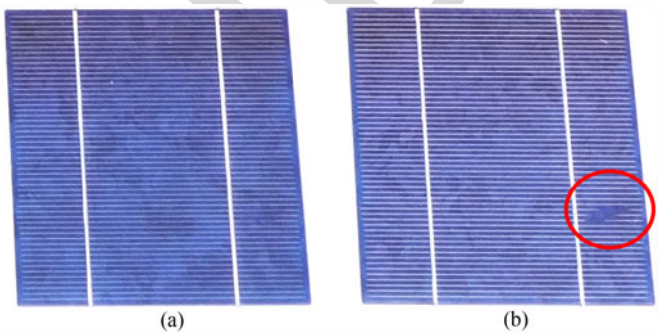

Fig. 9. Comparison among the state of the same PV cell. (a) year 2013 and (b) year 2015.

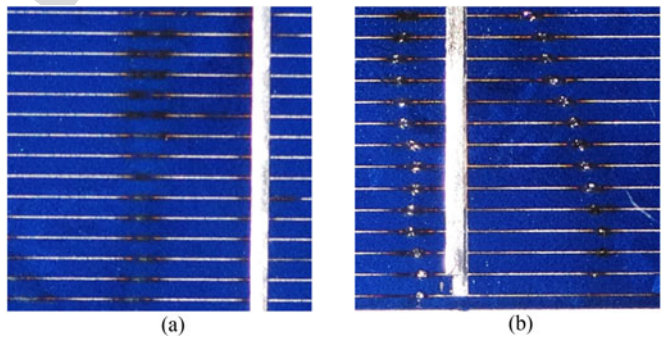

Fig. 10. Status of the fingers under the snail trails. (a) Year 2013 and (b) year 2015.

There is no clear explanation of this snail trail evolution. Over the two-year period, no further decrease of performance was observed, and only very minor evolution of new grid finger discoloration occurred. A localized hot spot caused by the high current density near the cracks in the PV cell can be the justification. Over time, the initial damage that looks like a burn evolves to a localized fusion of the metallic material, leading to a permanent damage of the cell and of the encapsulant. A microscopic change of "old" discoloration represents a reason that has to be investigated further.

Finally, it can be stated that snail trails are developing only at the beginning of outdoor operation and have no measureable long-term impact, which confirms the conclusions of [16].

VI. Conclusion

The analysis of PV modules degradation during their operation period is highly important for evaluating their performances. Several defect phenomena can appear immediately after installation and during their operation lifetime. Among these degradation effects, the snail trails and microcracks occurring in PV systems within several months after the installation are highly impacting the PV performances.

In this study, several tests were carried out to analyze some modules affected by snail trails phenomena. Tests such as the visual inspection, maximum power determination, dielectric withstand, and wet leakage current tests were carried out in a real-practice facility in Italy. MPP determination indicated a reduction by 10–30% with respect to datasheet figures. The indoor EL test showed a strong correlation between the occurrence of snail trail phenomenon and microcrack in PV cells: Snail trails indicate the presence of cell cracks.

Afterward, energy production tests were applied to four PV modules, by comparing their energy production with the one of a commercial PV modules used as reference, for the period April–August 2015. The obtained results highlight that the cell cracks can reduce the energy production of PV modules by 29% with respect to the reference PV module. The performance loss is correlated with the amount of cell cracks.

Finally, a comparison with the results obtained in a previous work was carried out to outline the long-term behavior of snail trails. Energy measurements and visual inspection showed limited evolution of the snail trails and, consequently, no significant variation in terms of power losses.

References

[1] M. Munoz, M. C. Alonso-Garcia, N. Vela, and F. Chenlo, "Early degradation of silicon PV modules and guaranty conditions," *Sol. Energy*, vol. 85, pp. 2264–2274, 2011.

[2] S. Djordjevic, D. Parlevliet, and P. Jennings, "Detectable faults on recently installed solar modules in Western Australia," *Renew. Energy*, vol. 67, pp. 215–221, Jul. 2014.

[3] A. Skoczek, "Long-term performance of photovoltaic modules," in *Proc. 2nd Int. Conf. Solar Photovoltaic Investments*, Frankfurt am Main, Germany, Feb. 2008, pp. 19–20.

[4] T. Sample, *Failure Modes and Degradation Rates From Field-Aged Crystalline Silicon Modules*. Golden, CO, USA: Nat. Renew. Energy Lab., NREL, Feb. 17, 2011.

[5] S. Meyer *et al.*, "Snail trails: Root cause analysis and test procedures," *Energy Procedia*, vol. 38, pp. 498–505, 2013.

[6] M. Köntges *et al.*, "Snail tracks (Schneckenspuren), worm marks and cell cracks," presented at the Proc. 27th Eur. Photovoltaic Sol. Energy Conf. Exhib., Frankfurt, Germany, 2012.

[7] S. Richter *et al.*, "Understanding the snail trail effect in silicon solar modules on structural scale," presented at the 27th Eur. Photovoltaic Sol. Energy Conf. Exhib., Frankfurt, Germany, 2012.

[8] S. Meyer *et al.*, "Silver nanoparticles cause snail trails in photovoltaic modules," *Sol. Energy Mater. Sol. Cells*, vol. 121, pp. 171–175, 2013.

[9] N. Kim *et al.*, "Analysis and reproduction of snail trails on silver grid lines in crystalline silicon photovoltaic modules," *Sol. Energy*, vol. 124, pp. 153–162, 2016.

[10] P. Peng *et al.*, "Microscopy study of snail trail phenomenon on photovoltaic modules," *RSC Adv.*, vol. 2, pp. 11359–11365, 2012.

[11] Y.-H. Lee *et al.*, "Indoor acceleration program for snail track effect in silicon solar modules," in *Proc. 28th Eur. Photovoltaic Sol. Energy Conf. Exhib.*, Paris, France, 2013, pp. 3135–3137.

[12] G. Stollwerck, W. Schoeppel, A. Graichen, and C. Jaeger, "Polyolefin backsheet and new encapsulant supress cell degradation in the module," in *Proc. 28th Eur. Photovoltaic Sol. Energy Conf. Exhib.*, Paris, France, 2013, pp. 3318–3320.

[13] M. Köntges, S. Kajari-Schroder, and I. Kunze, "Crack statistic for wafer based silicon solar cell modules in the field measured by UV fluorescence," *IEEE J. Photovoltaics*, vol. 3, no. 1, pp. 95–101, Jan. 2013.

[14] J. Käsewieter, F. Haase, and M. Köntges, "Model of cracked solar cell metallization leading to permanent module power loss," *IEEE J. Photovoltaics*, vol. 5, no. 6, pp. 1735–1741, Nov. 2015.

[15] A. Morlier, F. Haase, and M. Köntges, "Impact of cracks in multicrystalline silicon solar cells on PV module power—A simulation study based on field data," *IEEE J. Photovoltaics*, vol. 6, no. 1, pp. 28–33, Jan. 2016.

[16] H.-C. Liu, C.-T. Huang, W.-K. Lee, S.-S. Yan, and F. M. Lin, "A defect formation as snail trails in photovoltaic modules," *Energy Power Eng.*, vol. 7, pp. 348–353, 2015.

[17] A. Dolara, S. Leva, G. Manzolini, and E. Ogliari, "Investigation on performance decay on photovoltaic modules: Snail trails and cell microcracks," *IEEE J. Photovoltaics*, vol. 4, no. 5, pp. 1204–1211, Sep. 2014.

[18] [Online]. Available: www.solartech.polimi.it

[19] *Crystalline Silicon Terrestrial Photovoltaic (PV) Modules—Design Qualification and Type Approval*, IEC 61215, 2005.

[20] *Photovoltaic (PV) Module Safety Qualification—Part 2: Requirements for Testing*, IEC 61730-2, 2009.

[21] *Thin Film Terrestrial Photovoltaic (PV) Modules-Design Qualification and Type Approval*, IEC 61646, 2008.

[22] J. Wohlgemuth and S. Kurtz, "Photovoltaic module Qualification Plus testing," in *Proc. 40th IEEE Photovoltaic Spec. Conf.*, 2014, pp. 3589–3594.

[23] *Photovoltaic System Performance Monitoring. Guidelines for Measurement, Data Exchange and Analysis*, IEC 61724, 1999.

Q3

Alberto Dolara (S'09–M'13) received the M.S. and Ph.D. degrees in electrical engineering from the Politecnico di Milano, Milano, Italy, in 2005 and 2010, respectively.

He is currently an Assistant Professor with the Department of Energy, Politecnico di Milano. His research interests include traction systems, power quality, electromagnetic compatibility, and renewable sources.

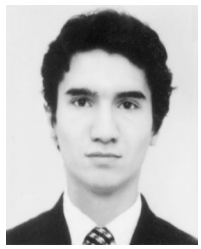

George Cristian Lazaroiu (SM'15) received the B.Sc. and M.Sc. degrees from the Department of Electrical Engineering, Politehnica University of Bucharest, Bucharest, Romania, in 2002 and 2003, respectively, and the Ph.D. degree in electrical engineering from the Politecnico di Milano, Milano, Italy, in 2006.

He is currently an Associate Professor with the Department of Power Systems, Politehnica University of Bucharest. His research interests include renewable energy sources, power electronics, and distributed energy resources.

Dr. Lazaroiu is a member of the Romanian Engineers Society (AGIR), the IEEE Power and Energy Society, the IEEE Industrial Electronics Society, and the IEEE Industry Applications Society.

Sonia Leva (M'00–SM'13) received the M.S. and Ph.D. degrees in electrical engineering from the Politecnico di Milano, Milano, Italy, in 1997 and 2001, respectively.

She is currently a Full Professor of electrical engineering with the Department of Energy, Politecnico di Milano. Her research interests include electromagnetic compatibility, power quality, and renewable energy analysis and modeling.

Dr. Leva is member of the IEEE Working Group "Distributed Resources: Modeling & Analysis," as well as the Task Force on "Modeling and Analysis of Electronically-Coupled Distributed Resources."

Giampaolo Manzolini received the M.S. degree in mechanical engineering and Ph.D. degree in energy from the Politecnico di Milano, Milano, Italy, in 2003 and 2007, respectively.

He is currently an Associate Professor with the Department of Energy, Politecnico di Milano. His research interests include energy conversion system optimization from fossil fuel and renewable energies, with particular attention to solar power systems.

Luca Votta received the M.S. degree in environmental and territorial engineering from the Politecnico di Milano, Milano, Italy, in 2006.

He is currently a Business Line Manager for solar energy with Kiwa Cermet Italia, Cadriano di Granarolo Emilia, Italy.

Mr. Votta is a member of the IEC-TC-82 Photovoltaic Energy (WG2), a member of CEI-CT-82 (WG1-WG2-WG13), and an IECRE member of the Solar PV Energy Working Group (WG 401).

QUERIES

Q1. Author: Please note that we cannot accept new source files as corrections for your paper. If possible, please annotate the PDF proof we have sent you with your corrections, using Adobe Acrobat editing software, and upload it via the Author Gateway. Alternatively, you may send us your corrections in a simple .txt file, utilizing the line numbers in the margins of the proof to indicate exactly where you would like for us to make corrections. You may, however, upload revised graphics via the Author Gateway.

Q2. Author: Figs. 5 and 6 are not cited in the text. Please cite them at appropriate places.

Q3. Author: Please provide full bibliographic details in Ref. [18].

Snail Trails and Cell Microcrack Impact on PV Module Maximum Power and Energy Production

Alberto Dolara, *Member, IEEE*, George Cristian Lazaroiu, *Senior Member, IEEE*, Sonia Leva, *Senior Member, IEEE*, Giampaolo Manzolini, and Luca Votta

***Abstract*—This paper analyzes the impact of the snail trail phenomena on photovoltaic (PV) module performances and energy production. Several tests (visual inspection, maximum power determination, dielectric withstand, wet leakage current, and electroluminescence test) were carried out on 31 PV modules located in a PV plant in Italy. The electroluminescence test highlighted the strong correlation between the appearance of snail trails and presence of damaged cells in PV modules. The daily energy produced by four PV modules affected by snail trails ranged between 68% and 88% of the energy produced by a damage free commercial PV module over the same period.**

***Index Terms*—Electroluminescence (EL), microcracks, photovoltaic (PV) modules, PV system reliability, snail trail phenomena.**

I. Introduction

THE direct use of solar energy for electrical energy production faced an intense development due to ongoing CO_2 emission reduction policies and the significant technical developments of photovoltaic (PV) technology. In addition, over the past decade, the cost production of PV cells has dropped, making electricity costs closer to conventional fuel costs. This development requires detailed evaluation of PV performances over lifetime to identify potential degradation phenomena [1]. Examples of degradation phenomena occurring in operating PV systems are encapsulant browning, delamination and bubble formation in the encapsulant, back sheet polymer cracks, front surface soiling, blackening at the bottom edge of the module, junction box connections corrosion, busbar oxidation and discoloration, junction cables insulation degradation, and glass breakage [2]–[4].

Among these, over the past few years, the "snail trails" (also known as worm marks or snail tracks) have been increasingly occurring in PV systems within few months after the installation. These effects appear on the front side or the edge of the solar cells [5], [6], such as a small narrow dark line and discoloration on the surface of the cell, [7], [8].

Manuscript received March 15, 2016; revised May 20, 2016; accepted May 25, 2016.

A. Dolara, S. Leva, and G. Manzolini are with the Department of Energy, Politecnico di Milano, Milano 20133, Italy (e-mail: alberto.dolara@polimi.it; sonia.leva@polimi.it; giampaolo.manzolini@polimi.it).

G. C. Lazaroiu is with the Department of Power Systems, Politehnica University of Bucharest, Bucuresti 060042, Romania (e-mail: cristian.lazaroiu@upb.ro).

L. Votta is with Kiwa Cermet Italia, 40057, Cadriano di Granarolo Emilia, Italy (e-mail: luca.votta@kiwacermet.it).

Color versions of one or more of the figures in this paper are available online at http://ieeexplore.ieee.org.

Digital Object Identifier 10.1109/JPHOTOV.2016.2576682

In previous works, the correlation between snail trail discolorations within the cells and cell microcracks was demonstrated. Meyer *et al.* performed chemical tests, Fourier transform infrared investigations, and X-ray photoelectron spectroscopy measurements on PV modules for snail trail defect analysis. Snail trails were correlated with chemical reactions occurring between silver of grid fingers and air humidity [5], [8]–[12].

Köntges *et al.* used fluorescence radiation to investigate micro cracks in PV cells, in order to determine the number, the position/orientation, and the frequency [13], [14]. Studies were further carried out in [15], simulating the PV module power affected by different crack types. The authors estimated that cracks isolate a cell section leading to a module strings power loss around 6–22%. They also suggested that the replacement of the most damaged module in a string allows a power recovery lower than the nominal power of a new module.

In [16], experiments to evaluate the impact of discolored lines like snail trails were performed both in laboratory and outdoor field, together with aging tests. A power reduction exceeding 5% was measured, and it was related to cell microcrack before snail trail formation.

This paper is a follow-up of a previous work [17] and investigates the performance of 31 PV modules under operation in a PV plant in Italy. The modules considered in this paper include also the four PV modules monitored in [17], where outdoor experiments on PV panels affected by snail trails outlined a reduction 1) in the photogenerated current, 2) of the shunt resistance in the electric equivalent circuit, and 3) of the energy production by 35%. Due to absence of some tests, no ultimate conclusions on the correlation between the snail trails phenomena and cells microcrack could be extended.

In this paper, several additional analyses were performed to highlight eventual issues besides visual defects as discoloration. The analyses are indoor visual inspection, maximum power determination, MST16 dielectric withstand, and wet leakage current. An important test carried out was the electroluminescence (EL) one, which allows correlating inactive ("broken") cell area and the level of performance loss. After the initial screening, the same modules considered in [17] were evaluated with long outdoor testing lasting five months 1) to compare the power and energy performances after two additional years of operation and 2) to assess the long-term behavior of cell cracks or snail trails under real operating conditions. The long-term observation of modules with grid finger discoloration is really a new contribution to this work, which, to the knowledge of the authors, was not previously investigated.

The experimental measurements were carried out at SolarTech^{LAB} [18], Politecnico di Milano, Italy.

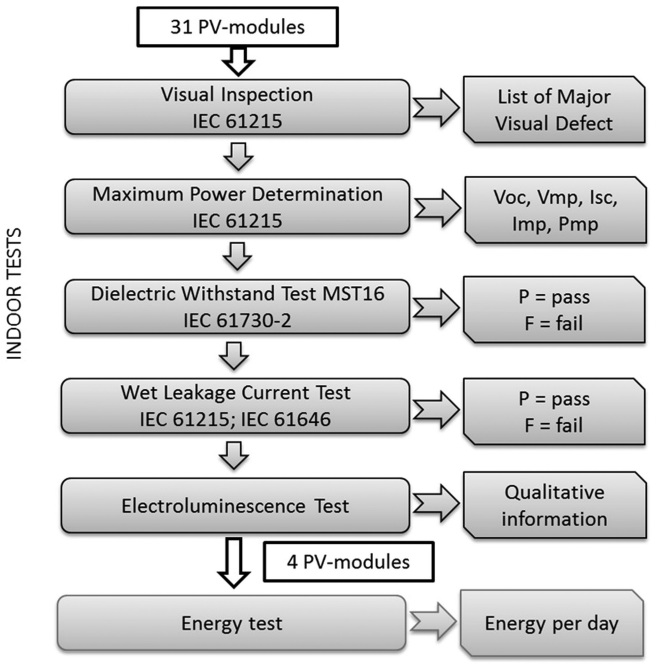

Fig. 1. Experimental procedure flowchart.

The paper is organized as follows: Section II describes the experimental procedures and the conducted tests. Section III reports the indoor experimental results, while Section IV reveals the energy experimental results for assessing snail trails effects on PV performances. In Section V, a comparison between the old and new outdoor measurements is presented. Section VI reports the final conclusions and the discussion of obtained results.

II. Experimental Procedure

The modules considered in this study were taken from a PV plant in operation. Among 4000 PV modules installed, 31 were selected by visual inspection: 16 modules affected by the snail trails at different rates and 15 with no trace of degradation.

As mentioned in [17], all the modules were manufactured in 2011 and have been operating since early 2012. Before their installation, each module performance was measured revealing good agreement with the corresponding datasheet, and no snail trail phenomenon or other issues were identified. After less than six months, these PV modules started to report a performance decay correlated with snail trail formation, since neither damages nor artificial breakage occurred. Performance decay was first evaluated in 2013 and, then, in 2015. During 2013–2015, the PV modules were in operation.

A multistep procedure (summarized in Fig. 1) was defined to assess the status and performances of the 31 modules. The procedure can be divided into two phases: the first one, named indoor tests, was carried out for all the modules, and the second one, named outdoor tests, for a limited number of modules. The following analyses were carried out.

A. Visual Inspection Tests

Visual inspection tests have been performed as defined by IEC 61215 [19]. For the purposes of design qualification and type approval, major visual defects were considered to be the following:

1) broken, cracked, or torn external surfaces, including superstrates, substrates, frames, and junction boxes;
2) bent or misaligned external surfaces, including superstrates, substrates, frames, and junction boxes to the extent that the installation and/or operation of the module would be impaired;
3) cracks, bubbles, or delaminations forming a continuous path between any part of the electrical circuit and the edge of the module;
4) loss of mechanical integrity, to the extent that the installation and/or operation of the module would be impaired.

B. Maximum Power Determination

The *I–V* characteristic curves were traced at standard test conditions (STC) in a sun simulator chamber of class AAA and *I–V* curve generator as defined by IEC 61215 [19]. The obtained results, at STC, were the following:

1) the open-circuit voltage V_{OC};
2) the voltage at maximum power point (MPP) V_{MPP};
3) the short-circuit current I_{SC};
4) the current at MPP I_{MPP};
5) the power at MPP P_{MPP}.

Using the maximum power value, the power variation (EFF) with respect to the nominal power value (i.e., indicated in the PV module datasheet) was calculated as follows:

$$\mathrm{EFF} = \frac{P_{\mathrm{MPP}} - P_N}{P_N} \cdot 100. \quad (1)$$

A negative value of EFF means a reduction in the power production with respect to the datasheet nominal power indicating possible problem in the module.

During MPP determination and EL tests, the electrical wires, connections, as well as the junction box or bypass diodes were also investigated to certify that they are undamaged and correctly operating.

C. MST16 Dielectric Withstand Test

This test is carried on at ambient temperature, according to the standard IEC 61730-2 [20], and at relative humidity not exceeding 75%. The module passes the test if there is no evidence of dielectric breakdown, or surface tracking, when a voltage equal to 2000 V plus four times the maximum voltage system is applied.

D. Wet Leakage Current Test

In agreement with the standards IEC 61215 [19] and IEC 61646 [21], the sample passes the test if the measured insulation resistance multiplied by the area of the module shall not be below 40 MΩ·m^2 (for modules with an area higher than 0.1 m^2).

TABLE I
OBTAINED RESULTS BY VISUAL INSPECTION AND MAXIMUM POWER DETERMINATION

#	P_N (W)	Finding – description	V_{OC} (V)	V_{MPP} (V)	I_{SC} (A)	I_{MPP} (A)	P_{MPP} (W)	*EFF*
1	220	Fingers blackened, scratch on cell, mark on cell. No major visual defects	24.5	19.7	8.25	7.53	148.4	-32.55%
2	220	Fingers blackened. No major visual effects	36.29	29.23	8.22	7.6	222	0.91%
3	230	Mark on cells, crack. No major visual defects	36.98	30.11	8.19	7.55	227.4	-1.13%
4	220	Fingers blackened. No major visual defects	36.35	29.17	8.25	7.57	220.7	0.32%
5	220	Fingers blackened. No major visual defects	36.27	29.18	8.18	7.59	221.4	0.64%
6	220	Mark on cells. Finger blackened. No major visual defects	36.35	29.24	8.16	7.71	225.3	2.41%
7	220	Fingers blackened. No major visual defects	24.09	19.42	8.23	7.59	147.3	-33.05%
8	220	Fingers blackened. No major visual defects	36.35	29.83	8.27	7.62	227.2	3.27%
9	220	Mark on cell. Fingers blackened. No major visual defects	36.32	29.23	8.34	7.69	224.8	2.18%
10	230	Fingers blackened, scratch on cell. No major visual defects	36.48	29.81	8.05	7.41	220.9	-3.96%
11	230	Fingers blackened. No major visual defects	36.87	30.18	8.28	7.68	231.8	0.78%
12	230	Scratch on cell. Finger blackened. No major visual defects	36.41	29.25	8.34	7.81	228.5	-0.65%
13	230	Fingers blackened. No major visual defects	36.39	29.87	8.2	7.53	224.9	-2.22%
14	230	Mark on cells. Fingers blackened. No major visual defects	36.48	29.25	8.29	7.88	230.5	0.22%
15	230	Mark on cell. Fingers blackened. Scratch on cells. No major visual defects	36.49	28.93	8.2	7.69	222.5	-3.26%
16	220	Several Snail Trails. Evidence of burning on cells and fingers	36.65	27.8	8.09	7.03	195.5	-11.14%
17	220	Several Snail Trails. Fingers blackened. Evidence of burning on cells	36.81	28.21	8	5.73	161.6	-26.55%
18	220	Several Snail Trails. Fingers blackened. Evidence of burning on cells	36.8	28.46	7.63	5.66	161.2	-26.73%
19	220	Several Snail Trails. Evidence of burning on cells. Fingers blackened	36.5	28.67	7.94	6.68	191.5	-12.95%
20	220	Evidence of burning on cells. Diverse snail trails. Fingers blackened	36.53	28.7	8.18	6.93	198.9	-9.59%
21	220	Several Snail Trails. Evidence of burning on cells. Fingers blackened	36.64	28.62	7.75	6.6	188.7	-14.23%
22	220	Several Snail Trails. Evidence of burning on cells	36.47	28.74	8.05	6.83	196.3	-10.77%
23	220	Several Snail Trails. Evidence of burning on cells. Fingers blackened	36.68	28.54	8.03	5.96	170.1	-22.68%
24	220	Several Snail Trails. Evidence of burning on cells. Fingers blackened	36.14	27.67	8.21	6.21	171.8	-21.91%
25	220	Several Snail Trails. Evidence of burning on cells. Fingers blackened	36.4	28.62	8.02	6.66	190.7	-13.32%
26	220	Several Snail Trails. Evidence of burning on cells. fingers blackened	36.47	28.64	8.07	6.41	183.5	-16.59%
27	220	Several Snail Trails. Evidence of burning on cells. Fingers blackened	36.52	28.78	7.94	5.82	167.5	-23.86%
28	220	Several Snail Trails. Evidence of burning on cells. fingers blackened	36.55	28.99	8.14	6.88	199.6	-9.27%
29	220	Several Snail Trails. Evidence of burning on cells. Fingers blackened	36.53	28.68	8.11	6.74	193.3	-12.14%
30	230	Evidence of burning on cells e Several Snail Trails	36.41	28.77	8.07	7.14	205.3	-10.74%
31	220	Several Snail Trails. Evidence of burning on cells. Fingers blackened. Cell chipped	36.69	27.39	8.16	6.48	177.4	-19.36%

E. Electroluminescence Test

The EL test is a qualitative test used, in particular, for detecting microcracks in PV modules. The affected areas are darker as they emit low or do not generate light emission. Thus, microcracks that are not visible, as well as broken contact fingers, can be identified. Sometimes, this test cannot be applicable (N/A) due to connection problems within the modules. In addition, for cracks not affecting the entire cell, future issues can be estimated if the module is further stressed (i.e., cracks electrically separating the major part of the cell) [1], [13], [14].

F. Energy Test

Four PV modules chosen among the ones with the lowest EFF were then analyzed under actual environmental conditions at the SolarTech$^{\text{LAB}}$ [18]. The irradiance availability in the site is calculated in terms of daily reference yield ($Y_{r,d}$). The energy produced by these PV modules was evaluated in terms of daily final yield index ($Y_{f,d}$) [22] and relative daily final yield ($RY_{f,d}$).

In agreement with the IEC 61724 [23], the daily reference yield $Y_{r,d}$ represents the number of peak sun-hours and is calculated as the global horizontal irradiance (GHI) in a day (kW h/m^2) divided by the reference irradiance (1 kW/m^2):

$$Y_{r,d} = \frac{\mathrm{GHI}_d(\mathrm{kWh/m^2})}{1(\mathrm{kW/m^2})}. \tag{2}$$

The index $Y_{f,d}$ is the energy output of the system divided by the peak power of the installed PV array at STC:

$$Y_{f,d} = \frac{E_{\mathrm{out},d}(\mathrm{kWh})}{P_N(\mathrm{kW})}. \tag{3}$$

The relative daily final yield is defined as the ratio between the final yield $Y_{f,d}$ of the PV modules under investigation, and the final yield $Y_{f,d\mathrm{REF}}$ of reference PV module:

$$RY_{f,d} = \frac{Y_{f,d}}{Y_{f,d\mathrm{REF}}} \cdot 100. \tag{4}$$

III. INDOOR EXPERIMENTAL TESTS RESULTS

The obtained results of the visual inspection and maximum power determination tests are summarized in Table I (the color label represents the difference between the PV module maximum power and the datasheet value: green indicates a positive or slight difference while red the highest power reduction). The PV modules #1 – #15 did not show significant visual defects. Indeed, no variation of maximum power of PV modules was measured, but for modules #1 and #7 which show a power reduction of about 33%. A further analysis related this reduction to some defects in the junction box connections, where one third of the module is disconnected and does not generate energy. The PV modules #16 – #31 had several snail trails deeply analyzed by EL tests with some fingers blackened in all the modules. Every module with discoloration due to snail trails has an MPP

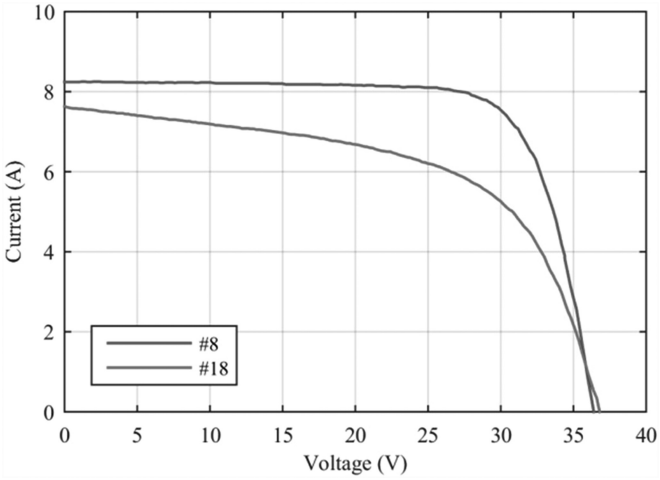

Fig. 2. Measured *I–V* curves of PV modules without major visual defects (#8) and with several snail trails (#18).

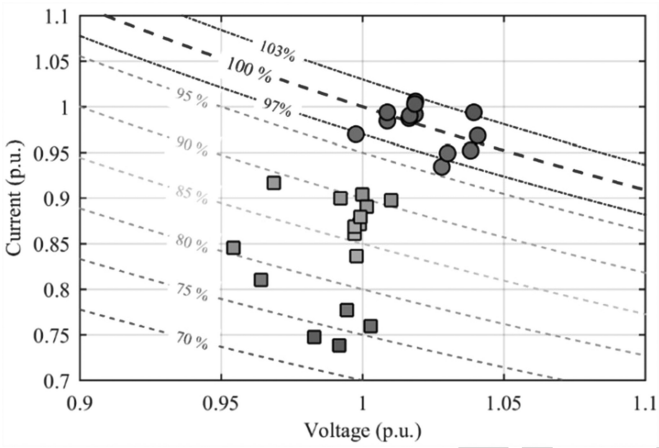

Fig. 3. MPP of the PV modules under analysis (except the one affected by diode failure) measured at STC in comparison with datasheet value (100%).

value below the nominal power; the reduction ranges from -9% to -27% with respect to the nominal power available from the datasheet.[1] In particular, a decay of the current at MPP can be outlined, while the $I_{\rm SC}$ and voltages are only marginally affected.

In Fig. 2, the measured *I–V* curves of two PV modules #8 and #18 are reported. The two curves show significant differences in the MPP, as well as resistance values: the shunt and series resistances in the equivalent electric circuit derived for the PV module #8 are 332.8 Ω, respectively, 0.4 Ω. For the PV module #18, the shunt resistance reduces to 23.6 Ω and the series resistance increases to 0.8 Ω. This is in agreement with the results reported in [17]. The same trend was outlined also for all the other modules affected by microcracks, but the graphs are not reported here for the sake of brevity.

Fig. 3 summarizes the voltage and current at MPP referred to the values indicated on the datasheet of the PV module.

[1]Some discrepancies occur between $P_{\rm MPP}$ reduction determined in this paper and in [17]. This may be due to the different adopted instrumentation, as well as test conditions (outdoor versus indoor).

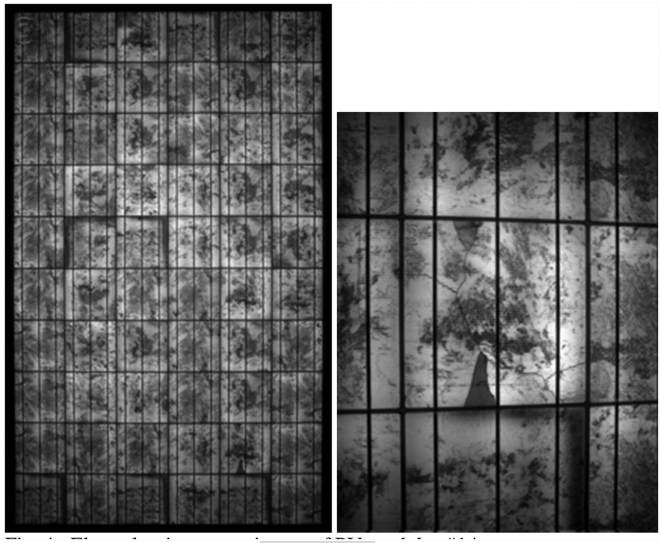

Fig. 4. EL image of PV modules #14.

The dashed lines are percentages of the maximum power. The modules not affected by snail trails are between or close to the blue-dashed lines, which represent the nominal power output $\pm 3\%$ of tolerance. Modules with snail trails have power output ranging from 75% to 90% of the nominal ones, which is mainly due to current density reduction.

In addition, all PV modules complied with the dielectric withstand test and wet leakage current test. Thus, there are no major anomalies in the electrical insulation of investigated PV modules, in dry and humid environment.

The last indoor test was the EL which was performed on all the modules. As a term of comparison, the EL image of a PV module without visual defects (#14) is reported in Fig. 4.

Among the 16 modules affected by snail trails, four among the ones with the lowest EFF were selected for the energy test at SolarTech$^{\rm Lab}$. The selected modules are #17, #18, #23, and #24 whose EL results are reported in Fig. 3, together with their visual imagery. Black areas in EL images represent electrically separated sections. The positions of cell are indicated in terms of coordinate (row, column) within the PV module, e.g., position (1,1) is on the left, top.

Starting from PV module #17, several snail trails are visible, e.g., in positions (3,1), (4,1), and (5,1). Furthermore, cracks are distinguishable in some cells located in positions (6,3) and (10,2). In addition, poor finger contacts are visible [see cell (5,4)]. Same considerations can be extended to the module #18 and #24, where snail trails are visible in cells (2,1), (2,2), and (3,3) in #18, while in #24, they are located in positions from (1,2) to (6,2). In addition, in these cases, poor finger contacts are present in cell (4,4) and position (6,1) and (7,1) in #18 and in #24, respectively.

In the case of PV module #23, several snail trails are visible, e.g., in position (1,5), (1,6), and (1,7); these correspond to electrically separated areas in EL images. Furthermore, cracks are distinguishable in some cells, e.g., in position (5,3). Again, poor finger contacts are visible, e.g., on cell (5,4), and not uniformity in light is present, e.g., on cells (7,4) and (5.3). For the module

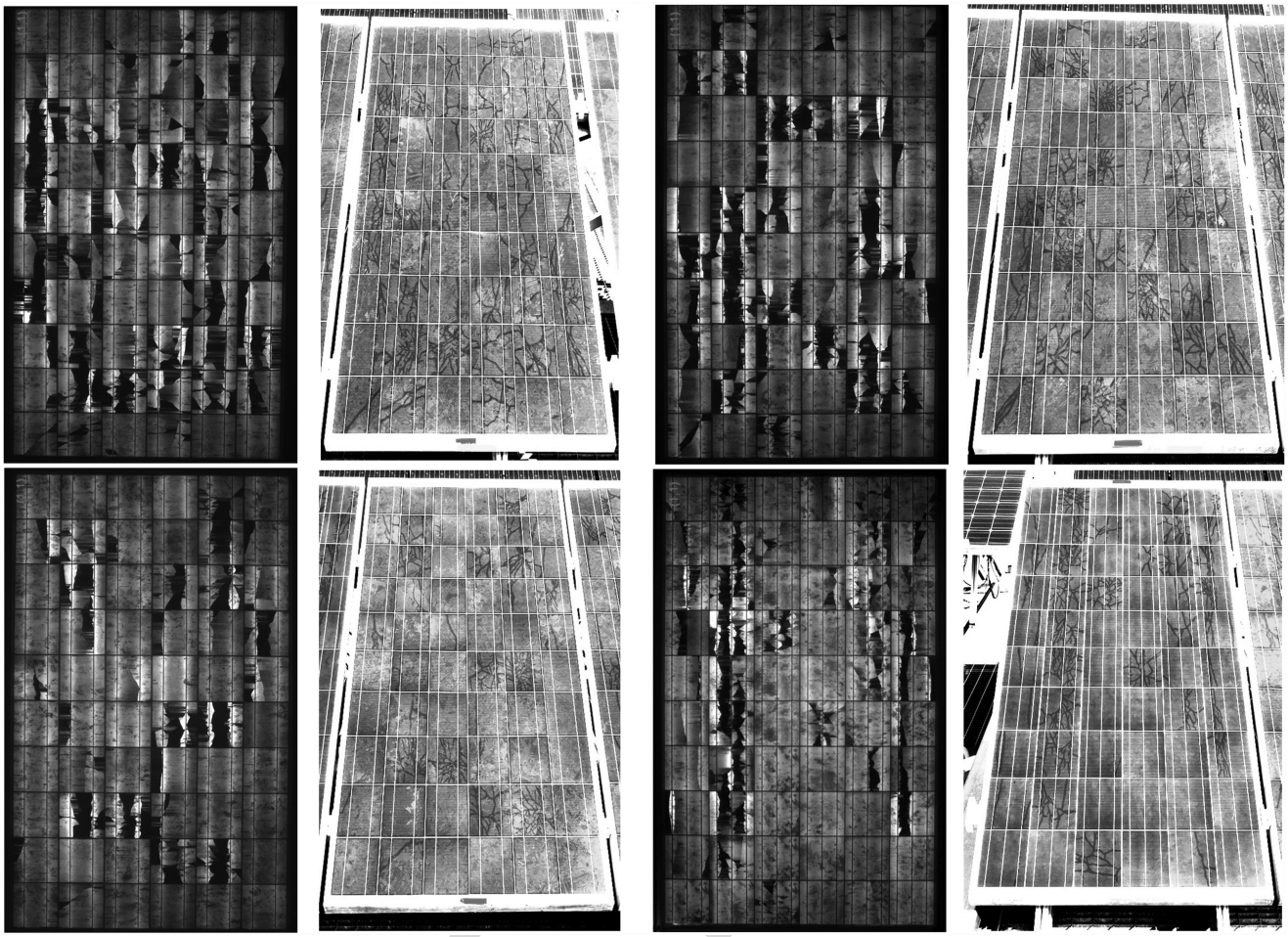

Fig. 5. EL image and picture of PV modules #17, #18, #23, and #24 starting from top-left.

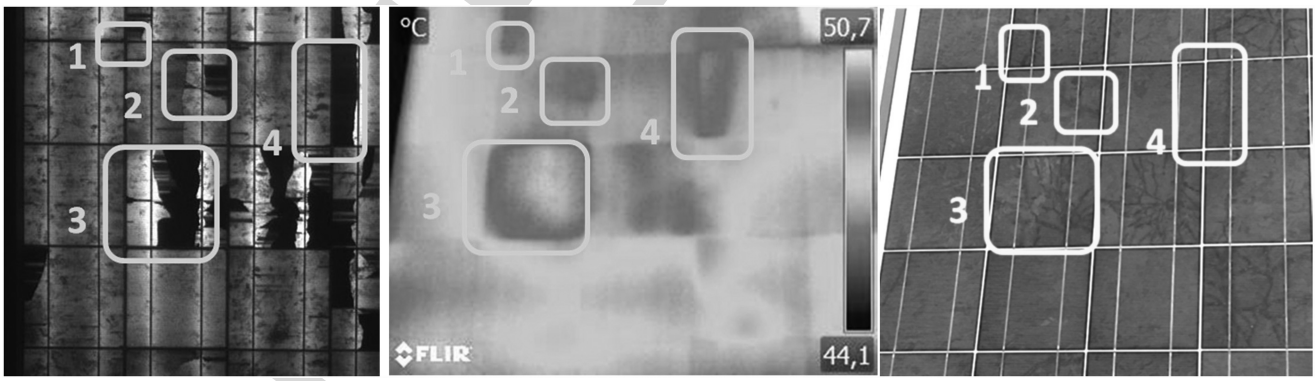

Fig. 6. EL, thermal, and visual imagines of #23 PV-module from (7,1) to (9,3) cells.

#23, in addition to EL analysis which outlined the same issues of the previous models, a thermal image together with EL and visual images of cells from (7,1) to (9,3) cells are shown in Fig. 4. Comparing the three images, it is possible to identify a link among visual defects, hot parts, and electrically separated areas.

In conclusion, the visual inspection carried on for all analyzed PV modules revealed the existence of various failures for 16 of them (#16 to #31), definitely ascribable to the phenomena known as "snail trails" on the PV modules under test. The EL test reveals the strong correlation between the appearance of snail trails and presence of damaged cells (microcracks) in PV modules. In addition, based on the experimental tests regarding determination of MPP, PV modules with significant cell breakage have a power reduction by 26–27% calculated at STC with respect to the manufacturer datasheet data.

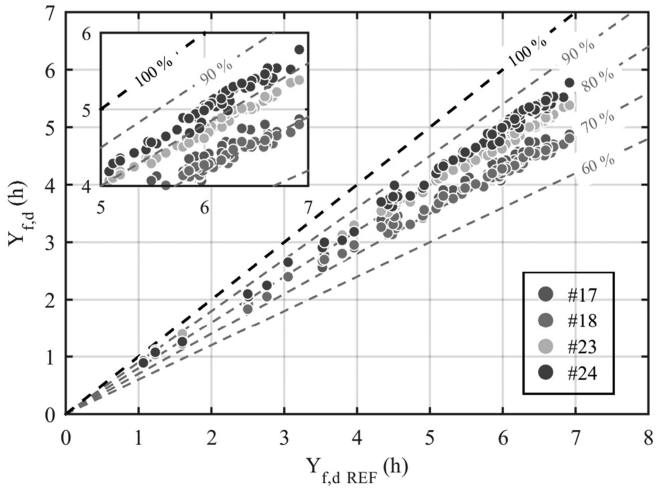

Fig. 7. Daily final yield of the PV modules #17, 18, 23, and 24 in the period April 2015–August 2015 referred to the daily final yield of the reference PV modules.

IV. Energy Comparison in SolarTech^{Lab}

An experimental campaign to evaluate the impact of snail trails on the energy production by PV modules was carried out. The objective of this experimental analysis was to assess the energy reduction due to snail trails and cell cracks phenomenon in some PV modules. MPP reduction is an indication about module performances at only one condition, while long-term energy analysis provides more insight about the status of the module affected by snail trails. In addition, the energy analysis is used to compare the module performance with previous results reported in [17]. The analysis focused on the total energy production over a period of four months.

The four PV modules #17, #18, #23, and #24 were installed at SolarTech^{Lab} [18] together with a commercial PV module (REFPV) of the same technology used as a reference case. The difference in aging was taken into account according to the datasheet information of the PV modules.

The continuous monitoring of the PV modules was conducted using the microinverter configuration adopted at the SolarTech^{Lab}. The inverters were previously characterized in terms of efficiency at different operating conditions, revealing a quite uniform behavior. Therefore, a possible performance reduction of the analyzed plant could specifically be related to the PV module and not to the power conversion system.

The energy produced by the PV modules in the period from April 2015 to August 2015 was recorded to quantify the influence of snail trails/cracks in terms of daily and total energy within the conducted test period. The daily energy generation—in terms of final yield ($Y_{f,d}$)—by PV modules referred to the final yield of REFPV module ($Y_{f,d\mathrm{REF}}$) is summarized in Fig. 7. The energy generation of the REFPV module, in terms of equivalent hours at peak power, is the black-dashed line.

The daily charts prove that the four PV modules affected by snail trails have a lower final yield ($Y_{f,d}$) between 68% and 88% with respect to the REFPV module. Since the reduction is referred to a PV module installed in the laboratory, the decrease can be related to the snail trails phenomenon due to microcrack. Hence, microcracks affect the PV performances by reducing the electrical energy production.

Fig. 8 illustrates the variation of relative daily final yield index ($RY_{f,d}$) for the four affected PV modules (#17, #18, #23, and #24) for each measured day. As illustrated in Fig. 8, the performance decay is higher during high solar radiation days characterized by high $Y_{r,d}$. Table II summarizes the final yield and relative final yield for the different months and the entire period of analysis. It is important to underline that the numbers of days in which the data are available are different for each month. PV modules #17 and #18 presents the highest reduction in energy production by about 30% than the REFPV module. Modules #23 and #24 show a lower energy reduction: they produce about 20% less in term of energy than the REFPV. These results are similar to the ones obtained by the maximum power tests. Besides diverse measurement accuracies and references adopted (REFPV instead of datasheet), the energy analysis represent the average behavior of the module under real operating conditions, which can differ from the ones at MPP. The energy results outline that the average behavior cannot be easily predicted: two modules (#17 and #18) have an energy reduction higher than the one at MPP, while the opposite occurs for #23 and #24.

Finally, the indoor measurements are carried out at STC, while the outdoor measurements are made under real conditions and, hence, affected by variable weather.

V. Long-Term Behavior of Snail Trails

An additional comparison in terms of energy production and visual analysis between previous [17] and this work is carried out to assess the long-term reliability of PV modules affected by snail trails. The four PV modules under analysis in the period in between operated for a total in-plane solar insolation of about 2000 kWh/m^2; hence, they suffered aging by actual weather conditions (sun UV, rain, snowfalls, etc.).

Table III summarizes the energy production results in terms of RY_{F} index obtained in the two campaigns. No significant deviation in the behavior of the PV modules can be outlined. The small differences can be due to different duration of the measurement campaigns and to diverse weather conditions.

Furthermore, a comparison in terms of visual images was performed. The PV cell visual inspection outlined only minor variations from 2013 to 2015. In general, only one or two cells in each PV module showed new snail trails, affecting a very limited area of the PV cell. This can be seen in Fig. 9, where in 2015, a small defect, which was not present in 2013, has appeared in the bottom right area of the PV cell.

Moreover, only in a few cells of each module, a variation of the fingers close to the snail trails was observed moving from case a to case b.

1) *Case a:* Fingers are not interrupted, and there is only a color variation from metallic gray to black [see Fig. 10(a)].
2) *Case b:* Fingers look broken, and small metal agglomerates with spherical shape are present in the center of the finger [see Fig. 10(b)].

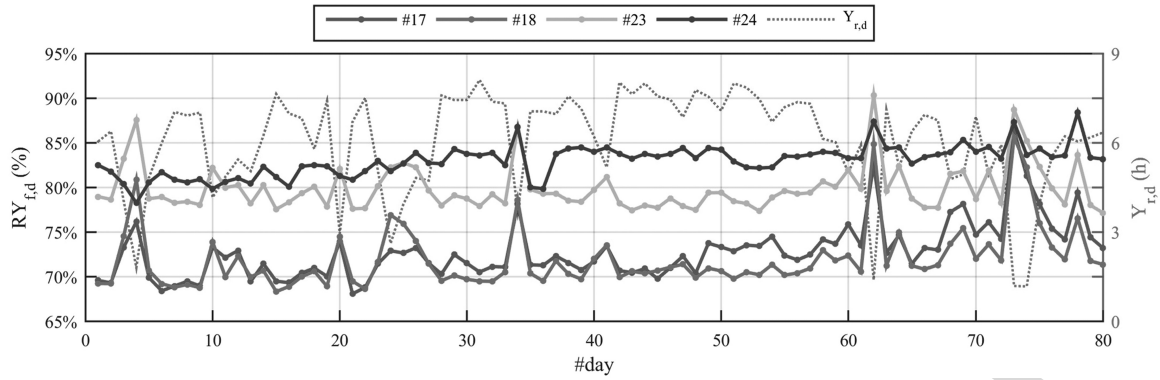

Fig. 8. Relative daily final yield index of the four PV affected modules #17, #18, #23, and #24 for 80 days in the period of analysis. The daily reference yield index for the same days has been reported on the secondarary *y*-axes.

TABLE II
MOTHLY AND TOTAL FINAL YIELD INDEX ($Y_{f,m}$) AND RELATIVE FINAL YIELD INDEX ($RY_{f,m}$) OF THE #17, #18, #23, AND #24 PV MODULES AND THE REFERENCE MODULE

			REFPV	#17		#18		#23		#24	
Month	Number of considered days	Solar irradiance (Wh/m^2)	$Y_{f,m}$ (h)	$Y_{f,m}$ (h)	$RY_{f,m}$	$Y_{f,m}$ (h)	$RY_{f,m}$	$Y_{f,m}$ (h)	$RY_{f,m}$	$Y_{f,m}$ (h)	$RY_{f,m}$
April	9	50.11	48.47	33.82	69.8%	33.96	70.1%	38.41	79.2%	39.31	81.1%
May	25	147.79	130.66	92.94	71.1%	92.43	70.7%	103.75	79.4%	107.59	82.3%
June	14	100.52	84.15	59.93	71.2%	59.52	70.7%	66.16	78.6%	70.12	83.3%
July	13	89.66	75.28	55.27	73.4%	53.38	70.9%	59.73	79.3%	62.72	83.3%
August	19	97.96	85.85	64.41	75.0%	62.77	73.1%	68.57	79.9%	72.22	84.1%
TOTAL	80	486.05	424.42	306.37	72.2%	302.05	71.2%	336.62	79.3%	351.96	82.9%

TABLE III
RELATIVE FINAL YIELD INDEX (RY_f) OF THE FOUR PV MODULES AFFECTED BY SNAIL TRAILS PHENOMENA FOR THE OLD AND NEW OUTDOOR MEASUREMENTS

PV Module	RY$_f$ [17][a] August 2013	RY_f April–August 2015
#17	68%	72%
#18	71%	71%
#23	77%	79%
#24	84%	83%

[A] RY_F was not adopted in [17]; hence, it was calculated starting from published numbers.

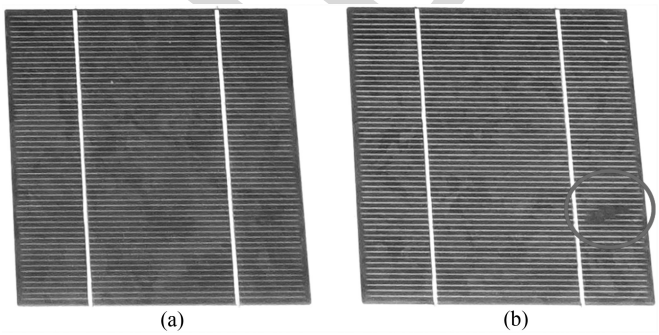

Fig. 9. Comparison among the state of the same PV cell. (a) year 2013 and (b) year 2015.

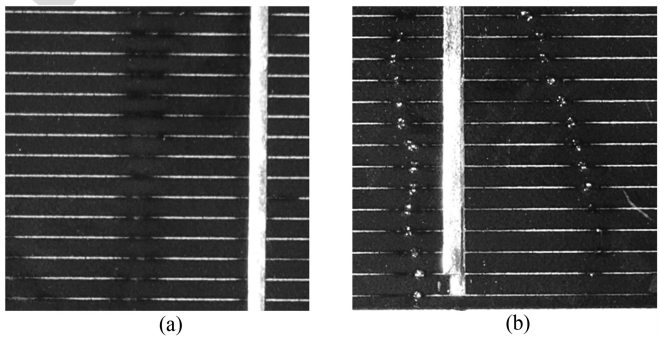

Fig. 10. Status of the fingers under the snail trails. (a) Year 2013 and (b) year 2015.

There is no clear explanation of this snail trail evolution. Over the two-year period, no further decrease of performance was observed, and only very minor evolution of new grid finger discoloration occurred. A localized hot spot caused by the high current density near the cracks in the PV cell can be the justification. Over time, the initial damage that looks like a burn evolves to a localized fusion of the metallic material, leading to a permanent damage of the cell and of the encapsulant. A microscopic change of "old" discoloration represents a reason that has to be investigated further.

Finally, it can be stated that snail trails are developing only at the beginning of outdoor operation and have no measureable long-term impact, which confirms the conclusions of [16].

VI. Conclusion

The analysis of PV modules degradation during their operation period is highly important for evaluating their performances. Several defect phenomena can appear immediately after installation and during their operation lifetime. Among these degradation effects, the snail trails and microcracks occurring in PV systems within several months after the installation are highly impacting the PV performances.

In this study, several tests were carried out to analyze some modules affected by snail trails phenomena. Tests such as the visual inspection, maximum power determination, dielectric withstand, and wet leakage current tests were carried out in a real-practice facility in Italy. MPP determination indicated a reduction by 10–30% with respect to datasheet figures. The indoor EL test showed a strong correlation between the occurrence of snail trail phenomenon and microcrack in PV cells: Snail trails indicate the presence of cell cracks.

Afterward, energy production tests were applied to four PV modules, by comparing their energy production with the one of a commercial PV modules used as reference, for the period April–August 2015. The obtained results highlight that the cell cracks can reduce the energy production of PV modules by 29% with respect to the reference PV module. The performance loss is correlated with the amount of cell cracks.

Finally, a comparison with the results obtained in a previous work was carried out to outline the long-term behavior of snail trails. Energy measurements and visual inspection showed limited evolution of the snail trails and, consequently, no significant variation in terms of power losses.

References

[1] M. Munoz, M. C. Alonso-Garcia, N. Vela, and F. Chenlo, "Early degradation of silicon PV modules and guaranty conditions," *Sol. Energy*, vol. 85, pp. 2264–2274, 2011.

[2] S. Djordjevic, D. Parlevliet, and P. Jennings, "Detectable faults on recently installed solar modules in Western Australia," *Renew. Energy*, vol. 67, pp. 215–221, Jul. 2014.

[3] A. Skoczek, "Long-term performance of photovoltaic modules," in *Proc. 2nd Int. Conf. Solar Photovoltaic Investments*, Frankfurt am Main, Germany, Feb. 2008, pp. 19–20.

[4] T. Sample, *Failure Modes and Degradation Rates From Field-Aged Crystalline Silicon Modules*. Golden, CO, USA: Nat. Renew. Energy Lab., NREL, Feb. 17, 2011.

[5] S. Meyer *et al.*, "Snail trails: Root cause analysis and test procedures," *Energy Procedia*, vol. 38, pp. 498–505, 2013.

[6] M. Köntges *et al.*, "Snail tracks (Schneckenspuren), worm marks and cell cracks," presented at the Proc. 27th Eur. Photovoltaic Sol. Energy Conf. Exhib., Frankfurt, Germany, 2012.

[7] S. Richter *et al.*, "Understanding the snail trail effect in silicon solar modules on structural scale," presented at the 27th Eur. Photovoltaic Sol. Energy Conf. Exhib., Frankfurt, Germany, 2012.

[8] S. Meyer *et al.*, "Silver nanoparticles cause snail trails in photovoltaic modules," *Sol. Energy Mater. Sol. Cells*, vol. 121, pp. 171–175, 2013.

[9] N. Kim *et al.*, "Analysis and reproduction of snail trails on silver grid lines in crystalline silicon photovoltaic modules," *Sol. Energy*, vol. 124, pp. 153–162, 2016.

[10] P. Peng *et al.*, "Microscopy study of snail trail phenomenon on photovoltaic modules," *RSC Adv.*, vol. 2, pp. 11359–11365, 2012.

[11] Y.-H. Lee *et al.*, "Indoor acceleration program for snail track effect in silicon solar modules," in *Proc. 28th Eur. Photovoltaic Sol. Energy Conf. Exhib.*, Paris, France, 2013, pp. 3135–3137.

[12] G. Stollwerck, W. Schoeppel, A. Graichen, and C. Jaeger, "Polyolefin backsheet and new encapsulant supress cell degradation in the module," in *Proc. 28th Eur. Photovoltaic Sol. Energy Conf. Exhib.*, Paris, France, 2013, pp. 3318–3320.

[13] M. Köntges, S. Kajari-Schroder, and I. Kunze, "Crack statistic for wafer based silicon solar cell modules in the field measured by UV fluorescence," *IEEE J. Photovoltaics*, vol. 3, no. 1, pp. 95–101, Jan. 2013.

[14] J. Käsewieter, F. Haase, and M. Köntges, "Model of cracked solar cell metallization leading to permanent module power loss," *IEEE J. Photovoltaics*, vol. 5, no. 6, pp. 1735–1741, Nov. 2015.

[15] A. Morlier, F. Haase, and M. Köntges, "Impact of cracks in multicrystalline silicon solar cells on PV module power—A simulation study based on field data," *IEEE J. Photovoltaics*, vol. 6, no. 1, pp. 28–33, Jan. 2016.

[16] H.-C. Liu, C.-T. Huang, W.-K. Lee, S.-S. Yan, and F. M. Lin, "A defect formation as snail trails in photovoltaic modules," *Energy Power Eng.*, vol. 7, pp. 348–353, 2015.

[17] A. Dolara, S. Leva, G. Manzolini, and E. Ogliari, "Investigation on performance decay on photovoltaic modules: Snail trails and cell microcracks," *IEEE J. Photovoltaics*, vol. 4, no. 5, pp. 1204–1211, Sep. 2014.

[18] [Online]. Available: www.solartech.polimi.it

[19] *Crystalline Silicon Terrestrial Photovoltaic (PV) Modules—Design Qualification and Type Approval*, IEC 61215, 2005.

[20] *Photovoltaic (PV) Module Safety Qualification—Part 2: Requirements for Testing*, IEC 61730-2, 2009.

[21] *Thin Film Terrestrial Photovoltaic (PV) Modules-Design Qualification and Type Approval*, IEC 61646, 2008.

[22] J. Wohlgemuth and S. Kurtz, "Photovoltaic module Qualification Plus testing," in *Proc. 40th IEEE Photovoltaic Spec. Conf.*, 2014, pp. 3589–3594.

[23] *Photovoltaic System Performance Monitoring. Guidelines for Measurement, Data Exchange and Analysis*, IEC 61724, 1999.

Alberto Dolara (S'09–M'13) received the M.S. and Ph.D. degrees in electrical engineering from the Politecnico di Milano, Milano, Italy, in 2005 and 2010, respectively.

He is currently an Assistant Professor with the Department of Energy, Politecnico di Milano. His research interests include traction systems, power quality, electromagnetic compatibility, and renewable sources.

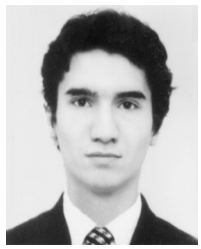

George Cristian Lazaroiu (SM'15) received the B.Sc. and M.Sc. degrees from the Department of Electrical Engineering, Politehnica University of Bucharest, Bucharest, Romania, in 2002 and 2003, respectively, and the Ph.D. degree in electrical engineering from the Politecnico di Milano, Milano, Italy, in 2006.

He is currently an Associate Professor with the Department of Power Systems, Politehnica University of Bucharest. His research interests include renewable energy sources, power electronics, and distributed energy resources.

Dr. Lazaroiu is a member of the Romanian Engineers Society (AGIR), the IEEE Power and Energy Society, the IEEE Industrial Electronics Society, and the IEEE Industry Applications Society.

Sonia Leva (M'00–SM'13) received the M.S. and Ph.D. degrees in electrical engineering from the Politecnico di Milano, Milano, Italy, in 1997 and 2001, respectively.

She is currently a Full Professor of electrical engineering with the Department of Energy, Politecnico di Milano. Her research interests include electromagnetic compatibility, power quality, and renewable energy analysis and modeling.

Dr. Leva is member of the IEEE Working Group "Distributed Resources: Modeling & Analysis," as well as the Task Force on "Modeling and Analysis of Electronically-Coupled Distributed Resources."

Giampaolo Manzolini received the M.S. degree in mechanical engineering and Ph.D. degree in energy from the Politecnico di Milano, Milano, Italy, in 2003 and 2007, respectively.

He is currently an Associate Professor with the Department of Energy, Politecnico di Milano. His research interests include energy conversion system optimization from fossil fuel and renewable energies, with particular attention to solar power systems.

Luca Votta received the M.S. degree in environmental and territorial engineering from the Politecnico di Milano, Milano, Italy, in 2006.

He is currently a Business Line Manager for solar energy with Kiwa Cermet Italia, Cadriano di Granarolo Emilia, Italy.

Mr. Votta is a member of the IEC-TC-82 Photovoltaic Energy (WG2), a member of CEI-CT-82 (WG1-WG2-WG13), and an IECRE member of the Solar PV Energy Working Group (WG 401).

QUERIES

Q1. Author: Please note that we cannot accept new source files as corrections for your paper. If possible, please annotate the PDF proof we have sent you with your corrections, using Adobe Acrobat editing software, and upload it via the Author Gateway. Alternatively, you may send us your corrections in a simple .txt file, utilizing the line numbers in the margins of the proof to indicate exactly where you would like for us to make corrections. You may, however, upload revised graphics via the Author Gateway.

Q2. Author: Figs. 5 and 6 are not cited in the text. Please cite them at appropriate places.

Q3. Author: Please provide full bibliographic details in Ref. [18].